



Contents lists available at ScienceDirect

Solid State Communications

journal homepage: www.elsevier.com/locate/sscMulti-carrier transport properties in *p*-type ZnO thin filmsH.B. Ye^a, J.F. Kong^a, W. Pan^a, W.Z. Shen^{a,*}, B. Wang^b^a Laboratory of Condensed Matter Spectroscopy and Opto-Electronic Physics, Department of Physics, Shanghai Jiao Tong University, 1954 Hua Shan Road, Shanghai 200030, China^b Department of Mathematics, Fudan University, 220 Han Dan Road, Shanghai 200433, China

ARTICLE INFO

Article history:

Received 13 May 2009

Accepted 23 June 2009 by X.C. Shen

Available online 30 June 2009

PACS:

73.61.Ga

73.50.Dn

73.50.Bk

Keywords:

A. Semiconductor

C. Impurities in semiconductors

D. Electronic transport

ABSTRACT

By the aid of temperature- and magnetic-field-dependent Hall effect measurements, we have extracted the multi-carrier transport information in N-doped and N–In codoped *p*-ZnO thin films grown on Si substrates through mobility spectrum analysis. It is found that owing to the compensation between free electrons and holes, the two-dimensional hole gas from ZnO/Si interface layers becomes determinant and results in the high *p*-type conductivity and high hole mobility in the ZnO samples. Compared with N-doping, the N–In codoping introduces many In donors and increases acceptor incorporation, as well as enhancing the free hole mobility due to the short-range dipole-like scattering.

© 2009 Elsevier Ltd. All rights reserved.

ZnO has generated a considerable amount of research activity over the past several years because of its emerging importance for fabricating short-wavelength optoelectronic devices, such as light-emitting diodes and laser diodes [1]. However, the growth of high quality *p*-ZnO has always been a difficult problem due to the asymmetric doping limitations in ZnO [2], and a great deal of effort has been made to realize the *p*-type ZnO, including single-doping and codoping with variable acceptor dopants and different substrates [3–9]. On the one hand, the most reported *p*-type ZnO films grown on insulating substrates have a mobility lower than 10 cm²/Vs with low conductivity of a weak *p*-type or *n*-type [3–6]. On the other hand, the *p*-ZnO films deposited on Si substrates exhibit high room-temperature hole mobility (even larger than 100 cm²/Vs) and high *p*-type conductivity [5–9]. In contrast to the great growth in interest, the understanding of the fundamental properties of *p*-ZnO is still relatively incomplete, especially for the carrier transport properties.

To date, the reported transport parameters of *p*-ZnO are all obtained by conventional Hall effect measurements at a single magnetic field, which provides only a weighted average of the carrier concentration and mobility. However, in the presence of multiple carrier species, there is often a lack of appreciation of the systematic errors when making these measurements and pitfalls occur in their interpretation and analysis. In order to

adequately explain the above different mobility characteristics observed in *p*-type doped ZnO films, alternative measurements and analysis techniques are required. The mobility spectrum analysis (MSA) is just an effective technique for treating magnetic-field-dependent Hall data, which can identify each carrier's type (hole or electron) origin, and the corresponding transport parameters in semiconductor materials [10].

In this paper, we have presented a comprehensive investigation of carrier transport properties in N-doped and N–In codoped *p*-ZnO thin films grown on Si substrates by ultrasonic spray pyrolysis (USP). Each carrier [bulk carriers and two-dimensional hole gas (2DHG)] has been extracted by the variable magnetic field Hall effect measurements in conjunction with the MSA and their effects on the electrical transport have been discussed. In addition, we have revealed the different doping mechanisms through the comparison of multi-carrier properties between N-doped and N–In codoped *p*-ZnO samples.

The studied N-doped and N–In codoped *p*-type ZnO thin films were deposited on intrinsic crystalline Si (100) substrates by USP at atmosphere [11]. Three kinds of aqueous solution, Zn(CH₃COO)₂ · 2H₂O (AR, 0.5 mol/l), CH₃COONH₄ (AR, 2.5 mol/l), and In(NO₃)₃ (AR, 0.5 mol/l), were chosen as the sources of zinc, nitrogen, and indium, respectively. The atomic ratio of Zn/N was 1:3 for the N-doped film, and Zn/N/In was 1:3:0.05 for the N–In codoped film, while the substrates were heated to 450 °C. The doping concentrations could be changed by the deposition rate and were realized in the range of 10¹⁷–10¹⁸ cm⁻³. All films were controlled to be 300 nm thick. Before electrical measurements, the ohmic contacts were fabricated by alloying indium on the

* Corresponding author. Tel.: +86 21 54743242; fax: +86 21 54741040.
E-mail address: wzshen@sjtu.edu.cn (W.Z. Shen).

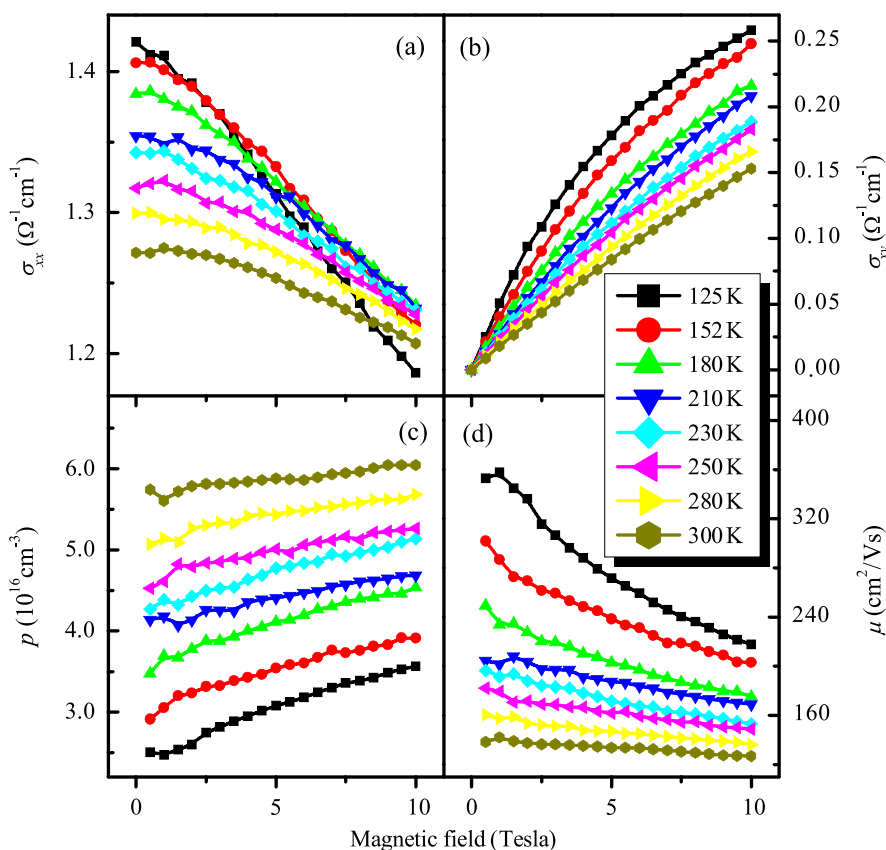


Fig. 1. Experimental conductivity tensors (a) σ_{xx} and (b) σ_{xy} as a function of magnetic field for N-doped *p*-ZnO measured from 125 to 300 K, together with the average carrier concentration p and mobility μ shown in (c) and (d).

surface of ZnO thin films and verified by the yielded linear and symmetric current–voltage characteristics. Magnetic-field-dependent Hall effect measurements were taken in the van der Pauw configuration under an Oxford Instruments superconductive magnet at temperatures ranging from 120 to 300 K and in a magnetic field up to 10 T.

Fig. 1(a) and (b) show the experimental conductivity tensors $\sigma_{xx}(B)$ and $\sigma_{xy}(B)$ as a function of magnetic field B for a typical N-doped *p*-ZnO thin film measured from 125 to 300 K. It can be seen that conductivity tensors both exhibit continuous changes with magnetic field and the positive values of $\sigma_{xy}(B)$ throughout 0–10 T reflects the *p*-type nature of the N-doped ZnO sample. According to the conductivity equations of $\sigma_{xx} = ep\mu/(1 + \mu B)^2$ and $\sigma_{xy} = ep\mu^2 B/(1 + \mu B)^2$ [10] which are valid for one type of carrier only, we present in Fig. 1(c) and (d) the average carrier concentration p and mobility μ derived from the experimental conductivity tensors. We note that the average carrier parameters (p and μ) alter gradually with the measured magnetic field, especially at low temperatures, which suggests that there must exist several baths of electrons and holes in the N-doped *p*-ZnO samples. In this case the average carrier concentration and mobility no longer represent the true transport information of the *p*-ZnO thin films.

In order to extract the multi-carriers existing in N-doped *p*-ZnO, we employ the MSA technique, which was proposed by Beck and Anderson [10] and further developed ten or more years later [12–15]. In the MSA technique, the mobility of the different carriers is assumed to be continuously distributed. Through the successive iterative algorithm in the MSA technique, we transform the experimental magnetic-field-dependent Hall data into the dependence of the conductivity density function on mobility, in which each carrier contributing to the total conductivity appears as a separate peak at a given mobility. The MSA technique has

the ability to deduce the type of all baths of carriers and their origin, concentration, and mobility. Fig. 2(a)–(d) illustrate the experimental magnetoconductivity tensors $\sigma_{xx}(B)$ (open squares) and $\sigma_{xy}(B)$ (open circles) for the N-doped *p*-ZnO sample at different temperatures of 300, 250, 180, and 125 K. The transport information of individual carriers has been extracted and shown as the corresponding mobility spectra in Fig. 2(a')–(d'), where their mobility and concentration can be determined by the peak value and area, respectively. The solid curves in Fig. 2(a)–(d) are the calculated conductivity tensors by the MSA, which are clearly in good agreement with the experimental data.

The MSA results shown in Fig. 2(a')–(d') all reveal three baths of electrons and holes in N-doped *p*-ZnO, which are electrons, low mobility holes, and high mobility holes. At $T = 300$ K, a mobility of $180 \text{ cm}^2/\text{V s}$ and concentration of $2.3 \times 10^{15} \text{ cm}^{-3}$ for electrons, and a mobility of $160 \text{ cm}^2/\text{V s}$ and concentration of $1.6 \times 10^{16} \text{ cm}^{-3}$ for low mobility holes are obtained from the mobility spectra in Fig. 2(a'). Here the intrinsic Si substrate has a very low conductivity of $2.94 \times 10^{-4} \text{ } \Omega^{-1} \text{ cm}^{-1}$. In our Hall experiment, two coplanar electrical contacts are formed on the ZnO thin films, where the electron transport will be influenced by the vertical potential of the ZnO/Si heterojunction. High potential exists at the interface of the heterojunctions, which blocks the electron vertical transport through the interface, resulting in the fact that the contribution of the substrate to the electrical conduction is negligible. Therefore, we can assign the above two carriers to the free electrons and holes from the ZnO thin films (denoted as e_{ZnO} and h_{ZnO}), respectively. Compared with the reported electron mobility of $205 \text{ cm}^2/\text{V s}$ in bulk ZnO [16], the mobility of free electrons in our ZnO films is a little smaller because of the polycrystalline nature. It should be noted that the most reported hole mobilities of smaller than $10 \text{ cm}^2/\text{V s}$ for *p*-ZnO are yielded through classic Hall effect

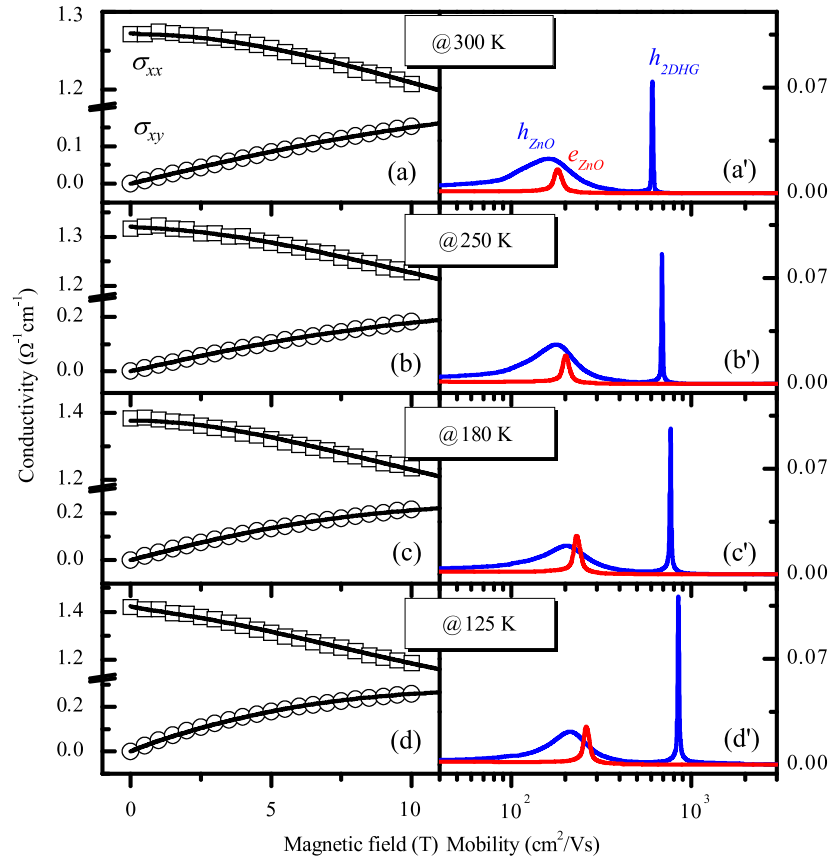


Fig. 2. Experimental conductivity tensors σ_{xx} and σ_{xy} as a function of magnetic field for N-doped *p*-ZnO at (a) 300, (b) 250, (c) 180 and (d) 125 K. The solid curves are the calculated results by using the mobility spectra in (a')–(d') derived from MSA.

measurements under a single magnetic field [3,4], and represent tradeoff results after taking into account the compensation of free electrons and holes. However, with the help of variable magnetic field Hall effect measurements followed by the MSA, we have the ability to separate the conductivity contributions of free electrons and holes in ZnO films. Therefore, the present transport parameters of free holes in N-doped *p*-ZnO are more reliable and exact. With the decrease of temperature, the increase in mobility of e_{ZnO} and h_{ZnO} can be observed, which is caused by the acoustic phonon scattering mechanism [16,17]. The mobility at 125 K for e_{ZnO} and h_{ZnO} is 260 and 210 $\text{cm}^2/\text{V s}$, respectively [see Fig. 2(d')].

Besides the bulk carriers from ZnO, anomalous high mobility ($>600 \text{ cm}^2/\text{V s}$) holes with narrow peaks have been observed from the corresponding mobility spectra in Fig. 2(a')–(d'). As no carrier in ZnO films can have such a high mobility, we attribute them to 2DHG (marked with $h_{2\text{DHG}}$) formed in the hole channel at ZnO/Si interfaces. This is due to the facts that an inversion layer is formed at the interface near the Si substrate, leading to the formation of the 2DHG [18], and, as stated above, the contribution of Si substrates to the electrical transport is negligible. When the temperature decreases from 300 to 125 K, the corresponding mobility increases from 610 to 850 $\text{cm}^2/\text{V s}$, indicating that the dominant mechanism at $T > 100 \text{ K}$ is acoustic phonon scattering. In addition, the 2DHG conductivity is found to decrease with the increase of temperature, while the free hole conductivity increases with the temperature. This observation indicates that the high mobility 2DHG moves gradually from the interface layer into the ZnO thin film.

To further confirm the multi-carrier analysis in *p*-ZnO and reveal the different doping mechanisms, we have performed magnetic-field-dependent Hall effect measurements on N-In codoped *p*-ZnO thin films grown on intrinsic Si substrates. Fig. 3 presents the typically derived conductivity tensors together with

the average carrier concentration and mobility as a function of magnetic field in the temperature range of 120–280 K. It is clear that the obvious changes of average carrier concentration and mobility with magnetic field are still present in N-In codoped ZnO, which also reveals the existence of multi-carriers in codoped *p*-ZnO. Nevertheless, in comparison with Fig. 1, the component $\sigma_{xx}(B)$ in N-In codoped ZnO exhibits an obvious increase with temperature while $\sigma_{xx}(B)$ in N-doped ZnO decreases instead. For the component $\sigma_{xy}(B)$, the variation trends with temperature are the same in both N-In codoped and N-doped ZnO, but the variation degree is different. These conduction behaviors suggest different carrier transport properties associated with doping mechanisms.

Fig. 4(a)–(d) display the experimental conductivity tensors (open symbols) and the fitted results (solid curves) from the MSA as a function of magnetic field for N-In codoped *p*-ZnO at temperatures of 280, 230, 160, and 120 K. The corresponding mobility spectra are illustrated in Fig. 4(a')–(d'), where three baths of electrons and holes denoted as e_{ZnO} , h_{ZnO} , and $h_{2\text{DHG}}$ are always observed. At $T = 280 \text{ K}$, the concentration and mobility for free electrons is $1.3 \times 10^{16} \text{ cm}^{-3}$ and 220 $\text{cm}^2/\text{V s}$, and for free holes is $7.2 \times 10^{16} \text{ cm}^{-3}$ and 130 $\text{cm}^2/\text{V s}$, as shown in Fig. 4(a'). The broad peak for free holes observed in all the studied *p*-ZnO is mainly due to the inhomogeneous doping of acceptor dopants as well as the effects of dislocations and defects. When at the low temperature of 120 K [see Fig. 4(d')], the mobility of free electrons and holes increases to 300 and 200 $\text{cm}^2/\text{V s}$, respectively. For the interfacial 2DHG, its mobility increases from 520 $\text{cm}^2/\text{V s}$ at 280 K to 900 $\text{cm}^2/\text{V s}$ at 120 K, still exhibiting the high mobility characteristic. All the temperature behaviors of mobility for the three carriers [e_{ZnO} , h_{ZnO} , and $h_{2\text{DHG}}$] in N-In codoped ZnO are consistent with the results in N-doped ZnO, indicating the reliability of our calculation and multi-carrier assignments.

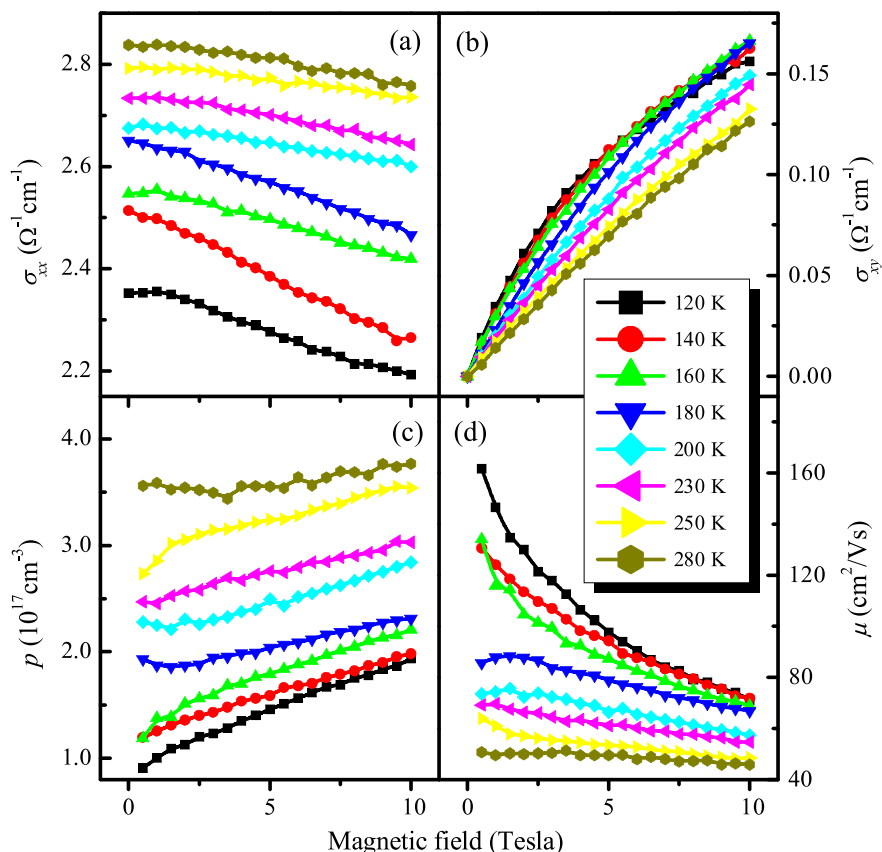


Fig. 3. Experimental conductivity tensors (a) σ_{xx} and (b) σ_{xy} as a function of magnetic field for N-In codoped *p*-ZnO measured from 120 to 280 K, together with the average carrier concentration p and mobility μ shown in (c) and (d).

Although Zhao et al. [18] suggested that the high *p*-type Hall conductivity in the ZnO/Si system was attributed to the interfacial 2DHG, they completely ignored the existence of free holes in ZnO films and simply regarded the ZnO films as *n*-type conductivity. Through the variable magnetic field Hall effect measurements followed by the MSA, we have confirmed and extracted the free electrons and holes from both the N-doped and N-In codoped ZnO films, together with the high mobility 2DHG from the interface layers between ZnO films and Si substrates. To our knowledge, this is the first report on the multi-carrier transport properties in *p*-ZnO. Because of the comparable conductivity between free electrons and holes in *p*-type doped ZnO, the existence of high mobility 2DHG becomes much significant and results in the high *p*-type conductivity and high hole mobility in the studied ZnO samples. Comparatively, the ZnO films grown on insulating substrates under the same growth conditions can only display weak *p*-type (the conductivity of free holes is larger than that of free electrons) or *n*-type (the conductivity of free holes is smaller than that of free electrons) conductivity with low mobility owing to the absence of 2DHG, which is consistent with the most experimental observation for *p*-type doped ZnO [3–6].

Finally, in order to reveal the different doping mechanisms, we have compared the multi-carrier transport properties between N-doped and N-In codoped *p*-ZnO. According to the mobility spectra shown in Fig. 2(a')–(d') and Fig. 4(a')–(d'), the enhancement of carrier concentration for free electrons and holes can be clearly observed in N-In codoped *p*-ZnO. In our previous work [11], we have calculated the donor and acceptor binding energy in different *p*-type doped ZnO from the temperature-dependent photoluminescence spectra and discussed the corresponding doping mechanisms. On the one hand, despite the N-In codoping

increases the donor binding energy, many In donors introduced by codoping at last lead to the increase of free electrons. On the other hand, the codoping technique can reduce the acceptor binding energy and enhance acceptor incorporation, thus the increase of free holes in N-In codoped *p*-ZnO is the clear evidence and demonstration. Additionally, the mobility of free holes in N-In codoped ZnO is also higher than those of N-doped ZnO, which is due to the short-range dipole-like scattering mechanism (long-range Coulomb scattering is dominant in the case of doping of acceptors alone) [2]. However, the different *p*-type doping in ZnO has no direct influence on the interfacial 2DHG. We should point out that these different characteristics for the three baths of electrons and holes with temperature result in the different temperature behaviors of conductivity observed in N-doped *p*-ZnO of Fig. 1(a)–(b) and N-In codoped *p*-ZnO of Fig. 3(a)–(b).

In summary, we have performed the magnetic-field-dependent Hall effect measurements on both N-doped and N-In codoped *p*-ZnO thin films grown on Si substrates by USP. By the aid of MSA, three baths of electrons and holes have been extracted, which are free electrons and holes from ZnO films, and the 2DHG from the interface layers between ZnO films and Si substrates. The broad structure for the free holes in ZnO films is caused by the inhomogeneous acceptor doping and different kinds of dislocations and defects. As a result of the comparable conductivity contributions between the free electrons and holes, the high mobility 2DHG leads to the high *p*-type conductivity and high hole mobility in the studied ZnO samples. In comparison with N-doped *p*-ZnO, the N-In codoping results in the increase of free electrons and holes due to many introduced In donors and enhanced acceptor incorporation, as well as the enhanced mobility of free holes attributed to the short-range dipole-like scattering.

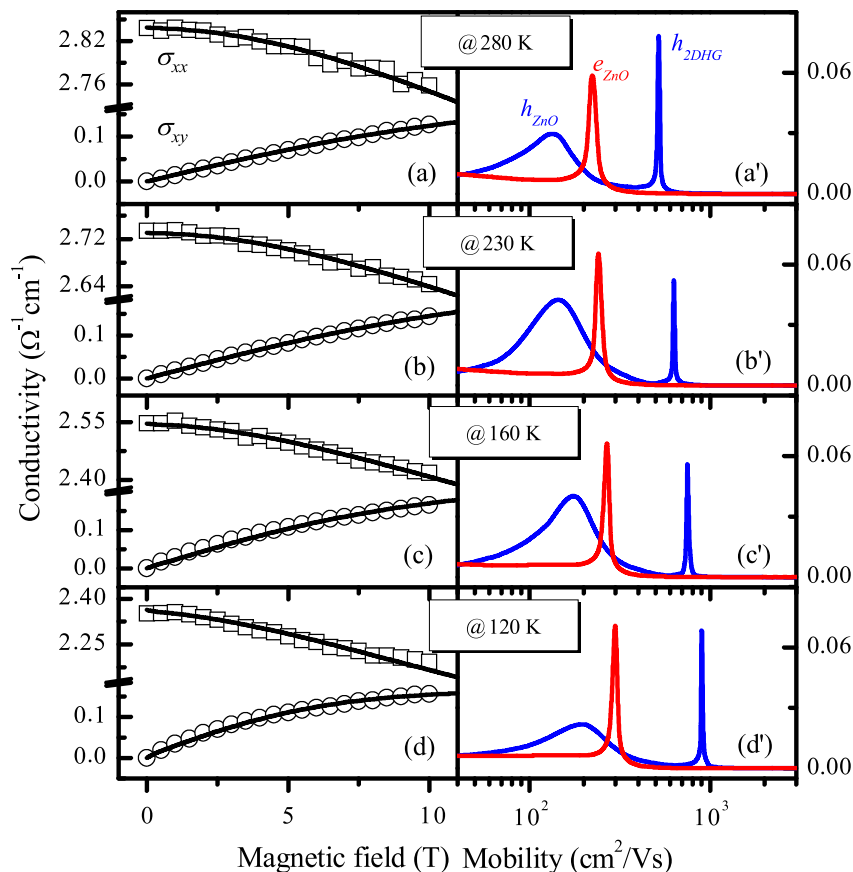


Fig. 4. Experimental conductivity tensors σ_{xx} and σ_{xy} as a function of magnetic field for N-In codoped *p*-ZnO at (a) 280, (b) 230, (c) 160 and (d) 120 K. The solid curves are the calculated results by using the mobility spectra in (a')–(d') derived from MSA.

Acknowledgements

This work was supported by the Natural Science Foundation of China (contract No. 10734020), National Major Basic Research Project of 2006CB921507, and Shanghai Municipal Commission of Science and Technology Project of 08XD14022. The authors would like to acknowledge Prof. X.M. Li for providing samples.

References

- [1] Ü. Özgür, Ya.I. Alivov, C. Liu, A. Teke, M.A. Reshchikov, S. Doğan, V. Avrutin, S.-J. Cho, H. Morkoc, *J. Appl. Phys.* 98 (2005) 041301.
- [2] T. Yamamoto, H. Katayama-Yoshida, *Physica B* 302/303 (2001) 155.
- [3] D.C. Look, D.C. Reynolds, C.W. Litton, R.L. Jones, D.B. Eason, G. Cantwell, *Appl. Phys. Lett.* 81 (2002) 1830.
- [4] J.G. Lu, Z.Z. Ye, F. Zhuge, Y.J. Zeng, B.H. Zhao, L.P. Zhu, *Appl. Phys. Lett.* 85 (2004) 3134.
- [5] F. Zhuge, L.P. Zhu, Z.Z. Ye, D.W. Ma, J.G. Lu, J.Y. Huang, F.Z. Wang, Z.G. Ji, S.B. Zhang, *Appl. Phys. Lett.* 87 (2005) 092103.
- [6] L.L. Chen, J.G. Lu, Z.Z. Ye, Y.M. Lin, B.H. Zhao, Y.M. Ye, J.S. Li, L.P. Zhu, *Appl. Phys. Lett.* 87 (2005) 252106.
- [7] J.M. Bian, X.M. Li, C.Y. Zhang, W.D. Yu, X.D. Gao, *Appl. Phys. Lett.* 85 (2004) 4070.
- [8] O. Lopatiuk-Tirpak, W.V. Schoenfeld, L. Chernyak, F.X. Xiu, J.L. Liu, S. Jang, F. Ren, S.J. Pearton, A. Osinsky, P. Chow, *Appl. Phys. Lett.* 88 (2006) 202110.
- [9] H.B. Ye, J.F. Kong, W.Z. Shen, J.L. Zhao, X.M. Li, *Appl. Phys. Lett.* 90 (2007) 102115.
- [10] W.A. Beck, J.R. Anderson, *J. Appl. Phys.* 62 (1987) 541.
- [11] H.B. Ye, J.F. Kong, W.Z. Shen, J.L. Zhao, X.M. Li, *J. Physica D: Appl. Phys.* 40 (2007) 5588.
- [12] Z. Dziuba, M. Gorska, *J. Phys. III* 2 (1992) 99.
- [13] J. Antoszewski, D.J. Seymour, L. Faraone, J.R. Meyer, C.A. Hoffman, *J. Electron. Mater.* 24 (1995) 1255.
- [14] I. Vurgaftman, J.R. Meyer, C.A. Hoffman, D. Redfern, J. Antoszewski, L. Faraone, J.R. Lindemuth, *J. Appl. Phys.* 84 (1998) 4966.
- [15] X.Y. Chen, W.Z. Shen, *Phys. Rev. B* 72 (2005) 035309.
- [16] D.C. Look, D.C. Reynolds, J.R. Sizelove, R.L. Jones, C.W. Litton, G. Cantwell, W.C. Harsch, *Solid State Commun.* 105 (1998) 399.
- [17] T. Makino, A. Tsukazaki, A. Ohtomo, M. Kawasaki, H. Koinuma, *Japan. J. Appl. Phys., Part 1* 45 (2006) 6346.
- [18] J.L. Zhao, X.M. Li, A. Krtschil, A. Krost, W.D. Yu, Y.W. Zhang, Y.F. Gu, X.D. Gao, *Appl. Phys. Lett.* 90 (2007) 062118.